PHYSICAL REVIEW A **84**, 032504 (2011)

Geometric Rényi divergence: A comparative measure with applications to atomic densities

J. Antolín,[1,3] P. A. Bouvrie,[2] and J. C. Angulo[2,3,*]

[1] *Departamento de Física Aplicada, EUITIZ, Universidad de Zaragoza, ES-50018 Zaragoza, Spain*
[2] *Departamento de Física Atómica, Molecular y Nuclear, Universidad de Granada, ES-18071 Granada, Spain*
[3] *Instituto Carlos I de Física Teórica y Computacional, Universidad de Granada, ES-18071 Granada, Spain*

(Received 18 May 2011; published 12 September 2011)

An alternative one-parameter measure of divergence is proposed, quantifying the discrepancy among general probability densities. Its main mathematical properties include (i) comparison among an arbitrary number of functions, (ii) the possibility of assigning different weights to each function according to its relevance on the comparative procedure, and (iii) ability to modify the relative contribution of different regions within the domain. Applications to the study of atomic density functions, in both conjugated spaces, show the versatility and universality of this divergence.

DOI: 10.1103/PhysRevA.84.032504 PACS number(s): 31.10.+z, 31.15.−p, 02.50.Cw

I. INTRODUCTION

Many information-theoretic divergence measures between two probability distributions have been introduced and extensively studied from their mathematical properties [1–5]. The applications of these measures can be found in the analysis of contingency tables [6], the approximation of probability distributions [7], signal processing [8], inference problems [9], pattern recognition [10], biodiversity [11], classification [12], homology [13], neural networks [14], computational linguistics [15], study of electronic densities [16–20], molecular similarity [21,22], texture and image registration [23], sequence analysis [24], machine learning [25], artificial intelligence [26], fuzzy set theory [27], and quantum-information theory [28], in particular as a measure of entanglement [29].

Among the proposed measures, the best known is the Kullback-Leibler [30] divergence based on Shannon entropy [31]. Since then, many other measures of divergence have been proposed and studied, in particular by using both local (Fisher) [32,33] and global (Shannon) [31] theoretic-information magnitudes. Some generalized entropies such as the Rényi one [34] have also been used to formulate deeper or more precise measures of discrepancy or distinguishability [35]. Applications of similarity and divergence measures to the study of atomic systems have been carried out in recent years, including the use of the quantum similarity index (QSI) [18] and the Jensen-Shannon divergence (JSD) [36].

The recent development in knowledge-based chemical research has created a surge of interest in chemical similarity or dissimilarity. Molecular modeling, molecular similarity [37], and quantitative structure activity relationship (QSAR) are simple examples of such an interest [38]. More recently the molecular quantum similarity framework has been used to provide a new set of quantum quantitative structure-properties relationship procedures (QQSPR) [39].

The aim of this work is to propose, study, and apply a new one-parameter generalized divergence measure, the geometric Rényi divergence (GRD$^{(q)}$), which has important advantages over other studied divergences. Such improvement mainly arises from the capability of GRD$^{(q)}$ to modify, by means of its characteristic parameter q, the relative contribution of relevant specific regions of the probability densities. The mathematical definition and properties of GRD$^{(q)}$ allow us to deal with arbitrary probability distributions, independently of their meaning or the specific fields of research, including all those previously mentioned.

We show the main properties of this divergence by comparing and studying a simple but highly hierarchical and organized set of quantum systems. We study the one-particle densities of atomic systems, in both conjugated spaces, which contain all the physical and chemical information through density-functional theory [40]. The obvious motivation is that the differences in the electronic charge densities of these species could be related to the differences in their respective physical and chemical properties, according to density-functional theory and the Hohenberg-Kohn theorem [41].

In this sense, especially remarkable are the applications carried out in this work by means of GRD$^{(q)}$, namely, (i) comparison among neutral atoms and interpretation in terms of shell-filling-patterns, (ii) study of ionization processes by analyzing the geometric divergence between the initial and final systems (neutral and cation) and its connection with the value of the ionization potential, (iii) study of divergence among densities, for a given system, computed with different models, and (iv) discrimination of whether an atom belongs to a set of systems with identical nuclear charges. The results here provided improve some of the aforementioned applications performed by using other measures, such as the quantum similarity index [18] or the Jensen-Shannon divergence [36]. Further applications to other systems and/or processes of physicochemical relevance (e.g., molecules and reactions) will be provided elsewhere.

The paper is organized as follows. In Sec. II we define the geometric Rényi divergence, showing its main mathematical properties. Section III is devoted to the application of GRD$^{(q)}$ to the study of one-particle densities of atomic systems, and in Sec. IV we summarize the main results of this work.

II. GEOMETRIC RÉNYI DIVERGENCE

The so-called Jensen-Rényi divergence (JRD$^{(q)}$) was first conceived [42] as a measure of dissimilarity or divergence

---

[*] Corresponding author: angulo@ugr.es

between two distribution functions, say $\rho_1(\vec{r})$ and $\rho_2(\vec{r})$, both of which are defined over the same d-dimensional domain $\Delta \in \mathbb{R}^d$. In doing so, the nonlinearity of the Rényi entropy [34]

$$R^{(q)}(\rho) \equiv \frac{1}{1-q} \ln \omega^{(q)}(\rho), \qquad (1)$$

according to the properties of the qth-order frequency moments

$$\omega^{(q)}(\rho) \equiv \int_\Delta \rho^q(\vec{r})\, d\vec{r}, \qquad (2)$$

was taken into account. In this way, the deviation from linearity allows us to define the Jensen-Rényi divergence between two distributions as [42]

$$\mathrm{JRD}^{(q)}(\rho_1,\rho_2) = R^{(q)}\left(\frac{\rho_1+\rho_2}{2}\right) - \frac{1}{2}[R^{(q)}(\rho_1) + R^{(q)}(\rho_2)], \qquad (3)$$

which constitutes the difference between the Rényi entropy of the arithmetic mean and the arithmetic mean of the respective Rényi entropies of ρ_1 and ρ_2. Generalizations of this divergence have been provided very recently [35] by considering mean values for an arbitrary number of distributions and their associated weights:

$$\text{‘}\mathrm{JRD}^{(q)}(\rho_1,\ldots,\rho_n) = R^{(q)}\left(\sum_{k=1}^n \alpha_k \rho_k\right) - \sum_{k=1}^n \alpha_k R^{(q)}(\rho_k), \qquad (4)$$

with the weights verifying $\sum_{k=1}^n \alpha_k = 1$.

In what follows, the integration domain Δ will be omitted in the notation unless necessary, for the sake of simplicity. We will deal with normalized-to-unity distributions, a condition which can be expressed as $\omega^{(1)}(\rho) = 1$.

Regarding the definition of $\mathrm{JRD}^{(q)}$, any order $0 < q \neq 1$ can be considered, as far as the involved frequency moments converge. The limiting case $q \to 1$ provides the so-called Jensen-Shannon divergence [43,44], $\mathrm{JSD} = \mathrm{JRD}^{(1)}$, defined as above but in terms of the Shannon entropy $S(\rho) \equiv -\int \rho(\vec{r}) \ln \rho(\vec{r})\, d\vec{r}$ [31] instead of the Rényi one. This is due to the limiting equality $S = R^{(1)}$ among entropies.

However, an essential constraint in performing studies by means of $\mathrm{JRD}^{(q)}$ has been the necessary condition of considering the order q not above unity. The reason is that the non-negativity of $\mathrm{JRD}^{(q)}$ is guaranteed only for $q \leqslant 1$, while for $q > 1$ it does not have a definite sign. According to the interpretation of $\mathrm{JRD}^{(q)}$ as a measure of distance or divergence among distributions, we must avoid values below zero, as usually done for arbitrary metrics in a given space.

Let us recall Eqs. (1) and (4). We can express $\mathrm{JRD}^{(q)}$ in terms of frequency moments as

$$\mathrm{JRD}^{(q)}(\rho_1,\ldots,\rho_n) = \frac{1}{1-q} \ln \frac{\omega^{(q)}\left(\sum_{k=1}^n \alpha_k \rho_k\right)}{[\omega^{(q)}(\rho_1)]^{\alpha_1} \cdots [\omega^{(q)}(\rho_n)]^{\alpha_n}}. \qquad (5)$$

The non-negativity of $\mathrm{JRD}^{(q)}$ for $q < 1$ arises from the value above unity of the fraction within the logarithm. The same property of $\mathrm{JRD}^{(q)}$ for $q > 1$ would be verified in case of the fraction being below unity, what is not necessarily true.

To get a Rényi-like divergence measure, non-negative for arbitrary order, we apply a different procedure in the present work. The well-known generalized Hölder's inequality [45] establishes that

$$\left[\int (f_1 f_2)^m d\vec{r}\right]^{1/m} \leqslant \left[\int f_1^s d\vec{r}\right]^{1/s} \left[\int f_2^t d\vec{r}\right]^{1/t} \qquad (6)$$

for any $m,s,t > 0$ verifying $\frac{1}{m} = \frac{1}{s} + \frac{1}{t}$. An iterative use of the above inequality allows us to assert that

$$\left[\int (f_1 \cdots f_n)^m d\vec{r}\right]^{1/m} \leqslant \left[\int f_1^{p_1} d\vec{r}\right]^{1/p_1} \cdots \left[\int f_n^{p_n} d\vec{r}\right]^{1/p_n}, \qquad (7)$$

with $\sum_{i=1}^n \frac{1}{p_i} = \frac{1}{m}$. Through the identities $f_i = \rho_i^{q/p_i}$ for a given $q > 0$, we obtain

$$\int (g_1^{\lambda_1} \cdots g_n^{\lambda_n})^q\, d\vec{r} \leqslant \left(\int g_1^q d\vec{r}\right)^{\lambda_1} \cdots \left(\int g_n^q d\vec{r}\right)^{\lambda_n}, \qquad (8)$$

where $\lambda_i \equiv m/p_i$ summing up to unity as $\sum_{i=1}^n \lambda_i = 1$. We can now provide, for arbitrary $q > 0$, a quotient above unity and consequently with its logarithm being above zero. The logarithm of the quotient is expressed in terms of frequency moments as

$$\lambda_1 \ln \omega^{(q)}(\rho_1) + \cdots + \lambda_n \ln \omega^{(q)}(\rho_n) - \ln \omega^{(q)}\left(\rho_1^{\lambda_1} \cdots \rho_n^{\lambda_n}\right) \geqslant 0, \qquad (9)$$

or in terms of the Rényi entropies defined in Eq. (1) as

$$\mathrm{GRD}^{(q)}(\rho_1,\ldots,\rho_n) \equiv (q-1)\left[R^{(q)}\left(\rho_1^{\lambda_1} \cdots \rho_n^{\lambda_n}\right) - \sum_{i=1}^n \lambda_i R^{(q)}(\rho_i)\right] \geqslant 0, \qquad (10)$$

where the quantity $\mathrm{GRD}^{(q)}$ will be referred to as the geometric Rényi divergence of order q for the set of distributions $\{\rho_i\}$ with weights $\{\lambda_i\}$.

Some comments are in order:

(1) Let us notice the strong resemblance between the terms within brackets in Eq. (10) and those of the definition of the Jensen-Rényi divergence ($\mathrm{JRD}^{(q)}$) in Eq. (4). In fact, all terms associated with individual distributions are identical, the difference between both expressions being determined by the multicomponent term. That term corresponds to the frequency moment of the arithmetic mean of the distributions in the $\mathrm{JRD}^{(q)}$ case, while the geometric mean, instead, in $\mathrm{GRD}^{(q)}$.

(2) The additional factor $(q-1)$ guarantees the non-negativity of $\mathrm{GRD}^{(q)}$ for any $q > 0$, including the nonzero and finite-valued limiting case $q = 1$. Adding the same factor in the definition of $\mathrm{JRD}^{(q)}$ would not solve the problem of the indefiniteness of sign for $q > 1$, as will be shown in Sec. III A.

(3) A particular case of physical relevance is obtained for $q = 2$:

$$\mathrm{GRD}^{(2)}(\rho_1,\ldots,\rho_n) = \ln \frac{[D(\rho_1)]^{\lambda_1} \cdots [D(\rho_n)]^{\lambda_n}}{D\left(\rho_1^{\lambda_1} \cdots \rho_n^{\lambda_n}\right)}, \qquad (11)$$

where the functional $D(\rho)$ is the so-called disequilibrium, a measure of departure of the distribution from uniformity [46].

So, GRD$^{(2)}$ for a set of distributions is expressed in terms of the quotient between the geometric mean of their respective disequilibria and the disequilibrium of the geometric mean of the distributions. Let us mention that the disequilibrium plays a relevant role also in what concerns the concept of shape complexity [47,48] and its physical interpretation for atomic [49] and molecular [50] systems.

(4) For clarity, we give below the simplest case of two densities with uniform weights, namely,

$$\mathrm{GRD}^{(q)}(\rho_1,\rho_2) = (q-1)\big\{R^{(q)}(\sqrt{\rho_1\rho_2}) - \tfrac{1}{2}[R^{(q)}(\rho_1) + R^{(q)}(\rho_2)]\big\}, \qquad (12)$$

to be compared with Eq. (3). The arithmetic mean is replaced by the geometric one, obtaining a non-negative divergence measure after including the factor $(q-1)$.

(5) GRD$^{(q)}$ keeps other relevant properties of JRD$^{(q)}$, including (i) invariance under exchange of distributions, (ii) additivity, and (iii) reaching the minimal value zero if and only if all distributions are identical.

(6) Nevertheless, GRD$^{(q)}$ possesses an additional property not shared with JRD$^{(q)}$. The geometric divergence of a set of distributions is independent of the normalization of each one within the set. Such an invariance under changes of normalization also holds for JRD$^{(q)}$ as far as those changes are identical for all distributions. In this sense, the comparison among distributions established by means of GRD$^{(q)}$ is based on a dissimilarity according to the shapes of the distributions, rather than on sizes, masses, charges, or any other quantity for which normalization is relevant.

(7) The main usefulness of the geometric Rényi divergence arises from its ability to modify the relative contribution of specific regions within the domain of definition in obtaining the divergence value, by varying appropriately the order q. This is a fundamental feature in applications to atomic systems, as will be discussed in the numerical analysis performed in the next section.

An illustrative example will allow us to understand better the role played by the order q of GRD. Let us consider two one-dimensional Gaussians, one of them centered at the origin, $f(x) = e^{-x^2}$, and the other one centered at an arbitrary point, $g(x) = e^{-(x-a)^2}$. Both have identical long-range behaviors, but short-range dissimilarity will be determined by the amount of the shift a. We compute straightforwardly $\mathrm{GRD}^{(q)}(f,g) = a^2q/4$. We notice that for fixed $a \neq 0$, the geometric divergence increases as q does, because of the emphasis in the comparison based on short-range values. For any fixed q, the saturation $\mathrm{GRD}^{(q)}(f,g) = 0$ occurs for $a = 0$, that is, $f = g$.

III. NUMERICAL ANALYSIS WITH ATOMIC ONE-PARTICLE DENSITIES

The geometric divergence introduced in this work possesses useful features, especially relevant when compared to previous measures of divergence. Let us remark that, on the one hand, the characteristic parameter q (order) enables us to modify the relative contribution of specific regions for the comparative process among densities. On the other hand, its non-negativity makes possible the interpretation as a "mean distance" (not in a strict mathematical sense) among the distributions under comparison. The latter is true for any $q > 0$. Such is not the case for the pioneering measure of divergence built up by means of the Rényi entropy, namely, the Jensen-Rényi divergence. In Sec. II we mentioned that its non-negativity (necessary to be interpreted as a divergence) is guaranteed only for $q \leqslant 1$.

For illustration, both the Jensen-Rényi and the geometric Rényi divergences between the one-particle densities of neutral atoms He and Fr are displayed in Fig. 1 for $0 < q \leqslant 6$, in both position and momentum spaces. The one-particle densities of N-electron systems are defined from the wave function $\Psi(\vec{r}_1,\ldots,\vec{r}_N)$ and its Fourier transform $\tilde{\Psi}(\vec{p}_1,\ldots,\vec{p}_N)$ as follows:

$$\rho(\vec{r}) = \int |\Psi(\vec{r},\vec{r}_2,\ldots,\vec{r}_N)|^2 d\vec{r}_2\cdots d\vec{r}_N \qquad (13)$$

in position space, and

$$\gamma(\vec{p}) = \int |\tilde{\Psi}(\vec{p},\vec{p}_2,\ldots,\vec{p}_N)|^2 d\vec{p}_2\cdots d\vec{p}_N \qquad (14)$$

in momentum space. Computations of $\rho(\vec{r})$ and $\gamma(\vec{p})$ for neutral and ionized atomic systems will be done, throughout this section, by means of accurate near-Hartree-Fock wave functions [51,52]. Atomic units (a.u.) will be used.

It is observed in Fig. 1 that, as we should expect, GRD$^{(q)}$(He,Fr) remains positive (in both spaces) within the whole interval, in fact, for any $q > 0$. However, JRD$^{(q)}$(He,Fr) reaches negative values for values of the order q above unity. In this example, negativity of the Jensen-Rényi divergence is observed for $q \geqslant 1.26$ in position space, and $1.08 \leqslant q \leqslant 3.00$ in the momentum one. Let us notice the existence of values of q for which JRD$^{(q)}$(He,Fr) = 0, in spite of dealing with two different distributions. So, the requirement of having null divergence if and only if the distributions under comparisons are identical is also violated.

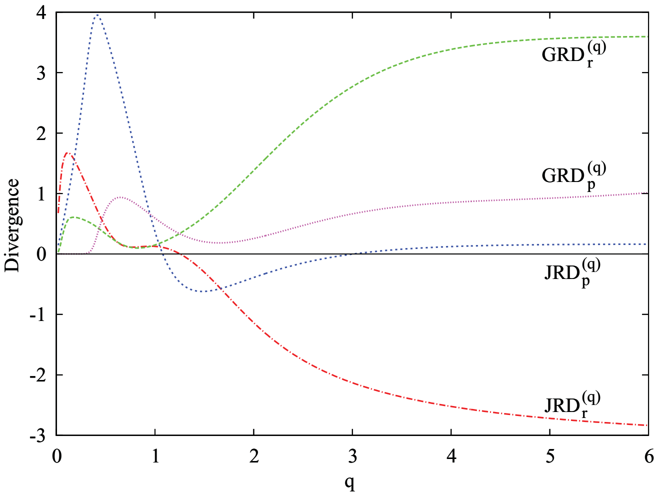

FIG. 1. (Color online) Jensen-Rényi (JRD$_r^{(q)}$) and geometric Rényi (GRD$_r^{(q)}$) divergences between charge densities of He and Fr neutral atoms, for $q = 0.4$ and $q = 2$.

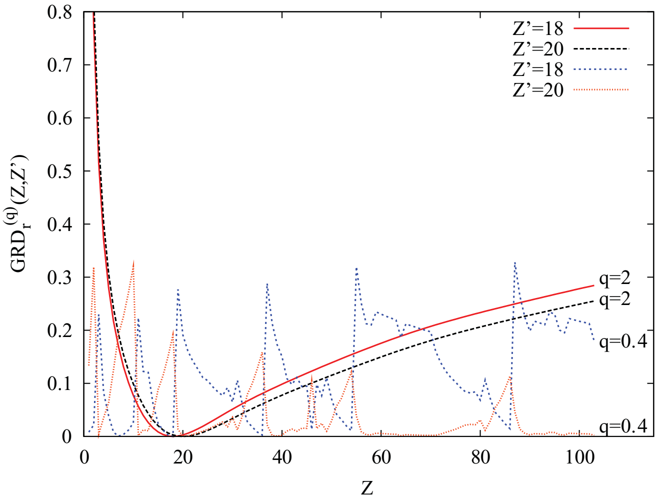

FIG. 2. (Color online) $\mathrm{GRD}_r^{(q)}(\mathrm{Ar},Z)$ and $\mathrm{GRD}^{(q)}(\mathrm{Ca},Z)$ in position space, for $q=0.4$ and $q=2$ of both argon and calcium with respect to neutral atoms $1 \leqslant Z \leqslant 103$.

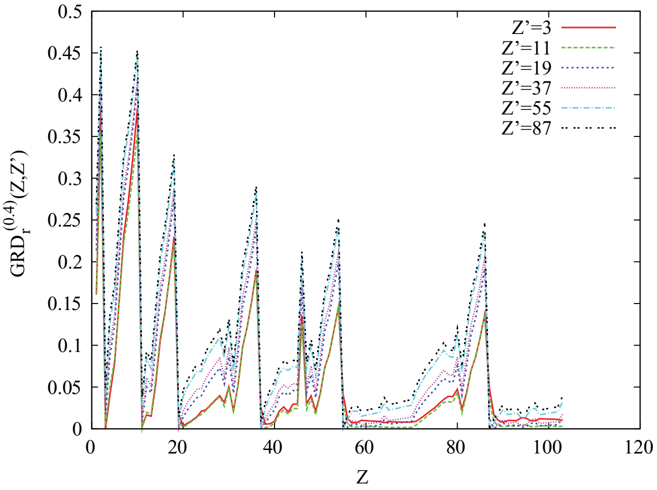

FIG. 3. (Color online) $\mathrm{GRD}_r^{(q)}(Z,Z')$ of order $q=0.4$, in position space, of each alkali metal ($Z'=3,11,19,37,55,87$) and neutral atoms $1 \leqslant Z \leqslant 103$.

A. Neutral atoms

The purpose of a study based on the divergence among atomic one-particle densities is to give an answer to the following question: to what extent is the similarity or divergence of those densities related to how similar or different the physical and chemical properties of the corresponding atomic systems are? The same question is appropriate in the frameworks of a great variety of scientific and technological fields, such as molecular systems, reaction processes, image registration, and analysis of DNA sequences.

Let us consider, at a first stage, two significantly different atoms, such as argon (a noble gas, nuclear charge $Z=18$) and calcium (an alkaline earth metal, $Z=20$). We compare, in Fig. 2, each of their charge densities $\rho(\vec{r})$ with all those of neutral atoms throughout the whole Periodic Table ($Z=1$–103). In doing so, the uniformly weighted geometric Rényi divergence ($\mathrm{GRD}^{(q)}$) in Eq. (12) is employed for orders $q=0.4$ and $q=2$. Differences among the results obtained for each value of q are apparent: very "soft" and almost identical curves for both Ar and Ca are obtained with $q=2$, while numerous local extrema appear for $q=0.4$ with the structures of the curves being extremely different from one another.

To justify these results from a physical point of view, it is worth remarking that the main atomic physical and chemical properties are determined by the shell structure and, in particular, by the characteristics (quantum numbers, occupancy, etc.) of the outermost subshell (valence region). The computation of $\mathrm{GRD}^{(q)}$ requires the computation of the qth-order frequency moments of each density and also of their geometric mean. Due to the exponential long-range behavior of the atomic charge densities, the relative contribution of the outermost region to the computation of the integrals involved is very small compared to that of the core. Such a contribution can be enhanced by raising the density to a relatively small power, as done when considering frequency moments of lower orders. Diminishing the value of $q=2$ up to $q=0.4$ allows us to gain enough information regarding valence features such that $\mathrm{GRD}^{(q)}$ reveals in most cases whether the systems under comparison share the above-mentioned features (e.g., if they belong to the same group of the Periodic Table). However, the closeness between both curves for $q=2$ is due to the similar values of their nuclear charges (18 and 20), together with the enhancement, for the computation of integrals, of the surroundings of the nuclei, where the attractive potential governed by the nuclear charge Z determines (roughly) the shape and magnitude of the electronic cloud. A detailed discussion on the patterns for the appearance of extrema is carried out in the next figure.

Six curves are drawn in Fig. 3, corresponding to the position-space $\mathrm{GRD}_r^{(q)}$ with $q=0.4$ between each alkaline metal (group IA) and all neutral atoms with $1 \leqslant Z \leqslant 103$. The similar structure of all curves, appearing almost perfectly embedded, is clearly observed. A detailed analysis of the location of maxima and minima results in the following observations:

(1) An almost systematic appearance of local minima occurs when comparing any of the above-mentioned systems with another one belonging to its own group ($Z=3,11,19,37,55,87$). These minimum values should be interpreted as a low divergence among systems that share the fundamental features at the valence region and, consequently, have similar physicochemical properties. Those minima correspond to the main ones observed in Fig. 3.

(2) The opposite occurs when comparing alkali metals with noble gases, with higher values (local maxima) of divergence. Let us recall the predisposition of alkali metals for reactivity, while noble gases ($Z=2,10,18,36,54,86$) are conformed so as to keep their closed-shell structure. According to the meaning of the divergence measure here considered, a high divergence should be expected , based on the one-particle densities, when comparing a pair of systems that are so different from a physical point of view. The appearance of local maxima when comparing alkali-metal–noble-gas atoms is absolutely systematic now.

(3) A number of additional extrema, not so relevant as for the above discussed, appear in each curve. The systems corresponding to minima can be classified, roughly, in two

different groups: (i) non-alkali-metal systems with a unique electron at the valence subshell ($Z = 13,31,49,81$), and (ii) systems suffering from anomalous shell filling ($Z = 29,79,93$). This similarly occurs for maxima, some of them corresponding to (i) closed-subshell systems ($Z = 12,30,48,80$) and (ii) anomalous shell filling again ($Z = 42,44,46,58,64,90,97$).

In comparing a given system with all others throughout the Periodic Table, the structural features of the curves in position space, in what concerns the number and enhancement of extrema, are very apparent as far as q decreases. The opposite trend is observed in the momentum-space comparison, in the sense of having curves with a higher structure as far as q becomes higher. The reason for those trends in opposite spaces requires us again to consider the enhancement of the relative contributions of the valence and core regions.

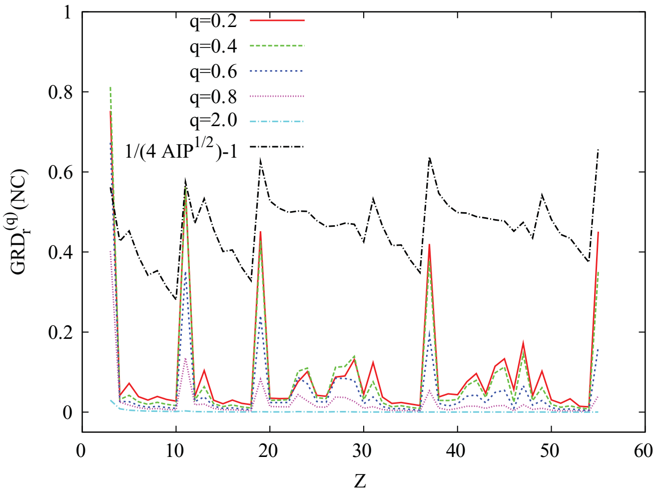

FIG. 4. (Color online) $\mathrm{GRD}_r^{(q)}(\mathrm{NC})$ between a neutral atom (N) and its singly-charged cation (C) with $3 \leqslant Z \leqslant 55$, and phenomenological correspondence with the atomic ionization potential (AIP) of the neutral system.

B. Ionization processes

Our next purpose is to analyze the effects arising from the physical process of atomic ionization, attending to the changes experienced by the one-particle densities of the system considered. In doing so, we employ the geometric Rényi divergence in order to compare the respective densities of the initial and final products (that is, the neutral atom and the singly charged cation) involved in this physical process. Within this context, we employ the notation $\mathrm{GRD}^{(q)}(\mathrm{NC})$ for the neutral-cation comparison in a given space.

For illustration, we consider the analysis in position space, i.e., for the quantity $\mathrm{GRD}_r^{(q)}(\mathrm{NC})$, with NC pairs of nuclear charges $3 \leqslant Z \leqslant 55$, and consequently each system containing a number of electrons up to 54. This quantity is displayed in Fig. 4 for different values of q, together with an algebraic function of the atomic ionization potential (AIP). This function of AIP is considered, instead of the actual AIP, in order to make easier the interpretation of the correlation observed among the divergence and AIP values.

In what concerns $\mathrm{GRD}^{(q)}(\mathrm{NC})$ for the considered q's, some comments are in order:

(1) Systems displaying (in Fig. 4) higher values (local maxima) of divergence between the neutral and ionized species can be classified as follows:

(a) $Z = 3,11,19,37,55$ (alkali metals) for which the ionization left empty the valence s subshell of the neutral atom, and the resulting cation possesses a closed-shell structure. These maxima occur in all curves with the exception of $q = 2$, a value too high to avoid the masking effect arising from the relatively sparse information on the valence features compared to the core ones.

(b) Similarly for $Z = 5,13,31,49$, but with the p subshell disappearing. The previous comment regarding the exception $q = 2$ applies also to these systems. Additionally, a d subshell becomes empty for $Z = 39$, but a value as low as $q = 0.2$ is needed r to detect it as a local maximum. Each of these systems provides (or not) a maximum according to the value of q.

(c) $Z = 8,16,34,52$ correspond to systems for which the outermost p subshell becomes half-filled. In this sense, we should emphasize the capability of $\mathrm{GRD}^{(q)}(\mathrm{NC})$ to discriminate systems with hall-filled valence subshells from others with a number of electrons (at the valence subshell) different from half the occupation number. These systems are displayed as maxima for all $q < 1$, while none for $q = 2$.

(d) Additional maxima are found for $Z = (23 \text{ or } 24)$, (one of $27,28,29$),$42,45,47$, depending on the curve. All these systems are characterized by an ionization process with the ejection of an electron from an inner s subshell, instead of the outermost one ($3d$ or $4d$). The only ones associated with maxima for $q = 2$ are $Z = 23,27,42$. The others require values of q below unity.

(2) The display of low divergence (some local minima) of divergence in Fig. 4 corresponds to closed-shell and closed-subshell systems ($Z = 4,10,12,18,30,3648,54$), the range of q for which they appear as minima depends on the specific systems considered. The subshell from which the electron is ejected remains occupied in the cation, and, consequently, changes in one-particle densities arising from the ionization are not so strong because of the presence of exactly the same occupied orbitals in the neutral atoms and its cation.

(3) There exists a clear resemblance between the divergence of pairs NC and the value of the AIP of the neutral system. The complete list of the 15 local minima of AIP for the systems here considered (displayed in Fig. 5 as maxima in the corresponding curve, due to the functional fit employed) is $Z = 3,5,8,13,16,19,23,28,31,34,37,47,49,55$. Let us notice that all these systems are included in the total list of high-divergence pairs.

To justify these results, let us notice that most systems with low AIP possess a valence subshell (independent of being the outermost one or not) containing a unique electron. Their ionization provokes the disappearance of that subshell, which translates in terms of changes experienced by the one-particle densities into a high value of the neutral-cation divergence.

Regarding the ionization analysis, we finally mention that similar conclusions to those here discussed, on the basis of the position-space densities, are obtained from the same analysis in momentum space.

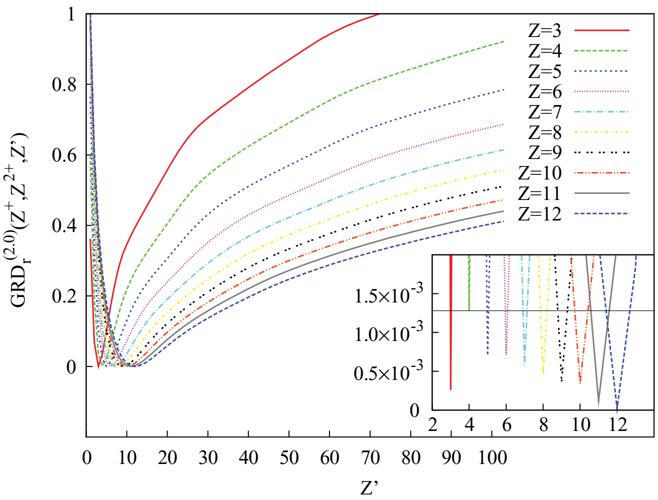

FIG. 5. (Color online) $\mathrm{GRD}_r^{(q)}(Z^+,Z^{2+},Z')$ among singly and doubly charged cations with nuclear charge $3 \leqslant Z \leqslant 12$, together with a neutral system of nuclear charge $1 \leqslant Z' \leqslant 103$. A threshold of GRD values appears amplified in the inset.

C. Further applications

1. Computational models

We consider the extent to which the use of more simplified or sophisticated models for computing the wave function provokes more or less significant differences among the corresponding one-particle densities. To give a well-posed answer, it is first necessary to establish a quantitative measure of difference among densities. The $\mathrm{GRD}^{(q)}$ divergence has been employed, both theoretically and numerically through this work, with the aim of quantifying how different two (or more) densities are.

In this sense, we could assert with a quantitative basis if, for instance, taking into account relativistic effects or correlations is worth doing in the study of multielectronic systems in terms of one-particle densities. Perhaps differences could be relevant when comparing wave functions, but not so important when dealing with densities. Similar analyses would be useful also for a comparative study of relevant distributions in physical systems (e.g., molecules and clusters), arising within different theoretical and/or numerical frameworks.

Let us analyze the effect of the interelectronic repulsion in the structural properties of the atomic charge and momentum densities. In doing so, we compute the densities using two different models: the accurate near-Hartree-Fock (HF) one employed for previous applications in this work, and the so-called bare Coulomb field (BCF) model [54], in which the interelectronic repulsive term of the Hamiltonian is neglected. This simplification provides a description of the multielectronic system as a superposition of hydrogenlike orbitals, in both spaces. The BCF system consists of a number of electrons within the attractive nuclear attraction, but noninteracting among themselves via repulsive forces.

Neglecting the interelectronic repulsion will provoke more or less significant changes in going from the HF situation to the BCF one. According to the previous description of these models, one should expect a more significant divergence among the HF and BCF densities as the number of electrons N increases (with $N = Z$ for neutral atoms, that is, those here considered). This would result from the much higher neglect of interelectronic repulsive forces that occurs for high N.

Certainly an increasing trend is observed for the HF-BCF divergence curves. However, none is strictly increasing, but local extrema appear whose number and enhancement depend on the order q considered. Locations of maxima and minima are determined by the shell structure, as also observed in the two previous applications. These comments apply in both spaces.

The main conclusion regarding the present comparison among densities computed within the HF and BCF models is that the effects of the interelectronic repulsion on the atomic one-particle densities depend not only on the total number of electrons but also on the shell-filling features of the systems considered.

2. Discrimination of nuclear charges

It is worth remembering the capability of the geometric Rényi divergence to quantify the divergence of a number of functions higher than 2. The interpretation as a "mean distance" among two or more functions remains, independent of the number of densities considered. For simplicity, we restricted all previous applications in this work to one-to-one comparisons.

Nevertheless, there exist additional applications of $\mathrm{GRD}^{(q)}$ among a set of distributions. We find it interesting to show one of them in the present work, but additional applications will be provided elsewhere.

Let us consider a number of atomic one-particle densities corresponding to systems sharing a specific property. Now we include in that set an additional distribution. A new question appears appropriate within this context: could we determine, in terms of the $\mathrm{GRD}^{(q)}$ values, if the system added to the initial set shares the specific features which characterize the initial set? We provide here an example for which $\mathrm{GRD}^{(q)}$ appears able to discriminate if the system added belongs or not to the initial set according to the features which characterize the set.

Consider a pair of cations with identical nuclear charge Z, one of them singly charged and the other doubly charged. We denote them as Z^{+1} and Z^{+2}, where the superscripts correspond to the respective global charges. Let us notice that a pair of systems as chosen above share the property of having the same nuclear charge Z. Now we add to this two-element set a third system: a neutral atom (global charge zero) with nuclear charge Z'. To perform the study of the uniformly weighted three-density divergence $\mathrm{GRD}_r^{(q)}(Z^{+1},Z^{+2},Z')$, we choose $q = 2$ for illustration. For the doubly charged ion, we use the near-Hartree-Fock wave functions of Ref. [53] for isoelectronic series with a number of electrons $N = 2$–10. They allow us to consider, for the present comparative purpose, values of the nuclear charges in the range $Z = 3$–12 for the systems comprising the initial set.

In Fig. 5, each curve corresponds to the election of Z for the initial two cations. Consequently, ten curves are displayed ($Z = 3$–12), each one as a function of $1 \leqslant Z' \leqslant 103$, the nuclear charge of the neutral atom added to the previous set. The first observation from Fig. 5 is the unimodal shape of all curves, decreasing quickly as Z' increases, until reaching a minimum value (which is shown amplified in the inset) and increasing hereinafter. It is observed that the absolute minima occur when $Z' = Z$ in each curve. The horizontal line establishes a threshold in the following sense: values of $\mathrm{GRD}_r^{(2)}(Z^{+1},Z^{+2},Z')$ above the aforementioned threshold allow us to assert that the neutral system added does not share the nuclear charge of the first two cations, that is, $Z' \neq Z$. However, any value below the line corresponds, necessarily, to the comparison of three systems with the same nuclear charge, which means that $Z' = Z$.

Summarizing this application, $\mathrm{GRD}^{(q)}$ has been shown to be a useful tool for discriminating atomic systems, in the sense of the ability to determine if a system added to a set of atoms characterized by some physical properties should belong to that set, or, in other words, if the new atom included in the set shares the properties common to all the others.

Further applications will be provided elsewhere. They should include (i) the use of different values of q, (ii) employment of weights other than the uniform ones, and (iii) a study based on properties (e.g., long-range behaviors) associated with the outermost regions, instead of the inner ones as done here.

IV. CONCLUSIONS AND OPEN PROBLEMS

An alternative measure of dissimilarity among probability distributions, the geometric Rényi divergence has been introduced in the present work. It is expressed in terms of the Rényi entropy, as also happens with the well-known Jensen-Rényi divergence. Both measures include a positive characteristic parameter in their definitions. The interpretation of JRD as a divergence measure constrains the parameter to values below unity, while no constraints at all are imposed on the GRD divergence.

The GRD statistical measure of divergence is used to compare atomic one-particle densities. The capability of GRD to gain physical insight into the structural properties of many-electron systems has been shown. In doing so, we have taken advantage of its characteristic parameter in order to enhance or diminish the short- and long-range contributions in a divergence-based analysis. The geometric Rényi divergence allows us to deal with a set of an arbitrary number of density functions, assigning different weights to each one in accordance with their roles within the comparative purpose considered. For atomic systems, a study based on one-particle densities in both position and momentum spaces provides clearly an interpretation by means of shell structure.

A detailed numerical analysis clearly established the relationship between valence subshell properties of the systems under comparison and the GRD values, as well as the detection of the presence of systems suffering from anomalous shell filling. The usefulness of the tool here defined has been shown in the study of ionized systems, by considering the analysis of atomic neutral-cation pairs. A strong resemblance appears among the extrema of divergence and those of the atomic ionization potential, mostly determined by occupancy numbers of the outermost subshell in neutral and cationic systems. Further applications of the generalized index, arising from its rigorous mathematical properties here described, have been carried out in this work, including studies (i) on the ability in comparing different quantum models, and (ii) detection of systems which do or do not share specific physical properties with their partners within an atomic set.

Additional studies are planned to be performed in a near future: (i) use of more sophisticated atomic models including relativistic effects and/or correlations, (ii) comparing more that two functions, e.g., sequence anion-neutral-cation, groups or periods of the Periodic Table, isoelectronic series, and subsystems of a given composite system, (iii) assigning appropriate weights to each system according to relevant physical and/or chemical properties, such as mass, number of electrons, and volume, and (iv) other quantum systems (e.g., molecules) and processes (reaction or excitation). It is worth remarking that the universality of GRD, in what concerns its definition and mathematical properties, allows its use in a wide variety of fields. systems, and processes, far beyond atoms, molecules, or reactions.

ACKNOWLEDGMENTS

This work was supported in part by the Spanish MICINN Project FIS-2008-02380, and the Grants No. FQM-4643 and No. FQM-2445 of Junta de Andalucía. The authors belong to the Andalusian research group FQM-020.

[1] J. Aczel and Z. Daroczy, *On Measures of Information and Their Characterizations* (Academic, New York, 1975).
[2] T. M. Cover and J. A. Thomas, *Elements of Information Theory* (Wiley Interscience, New York, 1991).
[3] J. Lin, IEEE Trans. Inf. Theory **37**, 145 (1991).
[4] I. J. Taneja and P. Kumar, Inf. Sci. **166**, 105 (2004).
[5] J. Briët and P. Harremoës, Phys. Rev. A **79**, 052311 (2009).
[6] D. V. Gokhale and S. Kullback, *Information in Contingency Tables* (Marcel Dekker, New York, 1978).
[7] C. K. Chow and C. N. Liu, IEEE Trans. Inform. Theory **14**, 462 (1968).
[8] Y. He, A. Ben Hamza and H. Krim, IEEE Trans. Signal Process. **51**, 1211 (2003).
[9] L. Pardo, *Statistical Inference Based on Divergence Measures* (Taylor and Francis, New York, 2005).
[10] X. Huang, S. Z. Li, and Y. Wang, *Proceedings of the IEEE Computer Society Conference on Computer Vision and Pattern Recognition (CVPR-2005)* **2**, 144 (2005).
[11] S. Pavoine, S. Ollier, and D. Pontier, Theor. Popul. Biol. **67**, 231 (2005).
[12] R. O. Duda, P. E. Hart, and D. G. Stork, *Pattern Classification* (Wiley, New York, 2001).
[13] S. Y. Chung and S. Subbiah, Structure **4**, 1123 (1996).
[14] K. Suzuki, H. Yamada, and S. Hasimoto, Pattern Recogn. Lett. **28**, 1104 (2007).

[15] P. Resnik, J. Artif. Intell. Res. **11**, 95 (1999).
[16] M. Ho, V. H. Smith Jr., D. F. Weaver, C. Gatti, R. P. Sagar, and R. O. Esquivel, J. Chem. Phys. **108**, 5469 (1998).
[17] S. Janssens, A. Borgoo, C. van Alsenoy, and P. Geerlings, J. Phys. Chem. A **112**, 10560 (2008).
[18] J. C. Angulo and J. Antolín, J. Chem. Phys. **126**, 044106 (2007).
[19] S. López-Rosa, J. Antolín, J. C. Angulo and R. O. Esquivel, Phys. Rev. A **80**, 012505 (2009).
[20] R. P. Sagar and N. L. Guevara, J. Mol. Struc.-Theochem **857**, 72 (2008).
[21] J. Cioslowski and A. Nanayakkara, J. Am. Chem. Soc. **115**, 11213 (1993).
[22] *Fundamentals of Molecular Similarity*, edited by R. Carbó-Dorca, X. Gironés, and P. G. Mezey (Kluwer Academic/Plenum, New York, 2001).
[23] B. Balas, Pattern Recogn. **41**, 972 (2008).
[24] P. Bernaola Galván, I. Grosse, P. Carpena, J. L. Oliver, R. Román-Roldán, and H. E. Stanley, Phys. Rev. Lett. **85**, 1342 (2000).
[25] G. Chechik, V. Sharma, U. Shalit, and S. Bengio, J. Mach. Learn. Res. **11**, 1109 (2010).
[26] P. Faratin, C. Sierra, and N. R. Jennings, Artif. Intell. **142**, 205 (2002).
[27] C. Zhang and H. Fu, Pattern Recogn. Lett. **27**, 1307 (2006).
[28] P. W. Lamberti, A. P. Majtey, A. Borrás, M. Casas, and A. Plastino, Phys. Rev. A **77**, 052311 (2008).
[29] A. P. Majtey, A. Borrás, M. Casas, P. W. Lamberti, and A. Plastino, Int. J. Quantum Inform. **6**, 715 (2008).
[30] S. Kullback and R. Leibler, Ann. Math. Stat. **22**, 79 (1951).
[31] C. E. Shannon and W. Weaver, *The Mathematical Theory of Communication* (University of Illinois, Urbana, IL, 1949).
[32] R. A. Fisher, Proc. Cambridge Philos. Soc. **22**, 700 (1925).
[33] B. R. Frieden, *Science from Fisher Information* (Cambridge University, Cambridge, England, 2004).
[34] A. Rényi, in *Proceedings 4th Berkeley Symposium on Mathematics, Statistics and Probability* (University of California, Berkeley, CA, 1961), Vol. 1, pg. 547.
[35] J. C. Angulo, S. López-Rosa, J. Antolín and R. O. Esquivel, Int. J. Quantum Chem. **111**, 297 (2011).
[36] J. Antolín, J. C. Angulo, and S. López-Rosa, J. Chem. Phys. **130**, 074110 (2009).
[37] R. Carbó-Dorca, J. Arnau, and L. Leyda, Int. J. Quantum Chem. **17**, 1185 (1980).
[38] R. Carbó-Dorca, L. Amat, E. Besalú, X. Gironés and D. Robert, J. Mol. Struct. **504**, 181 (2000).
[39] R. Carbó-Dorca and S. van Damme, Theor. Chem. Acc. **118**, 673 (2007).
[40] R. G. Parr and W. Yang, *Density Functional Theory of Atoms and Molecules* (Oxford University Press, New York, 1989).
[41] P. Hohenberg and W. Kohn, Phys. Rev. B **136**, 864 (1964).
[42] J. Burbea and C. R. Rao, IEEE Trans. Inf. Theory **28**, 489 (1982).
[43] A. K. C. Wong and M. You, IEEE Trans. Pattern Anal. Machine Intell. **7**, 599 (1985).
[44] C. R. Rao and T. Nayak, IEEE Trans. Inf. Theory **31**, 589 (1985).
[45] A. W. Marshall and I. Olkin, *Theory of Majorization and Its Applications* (Academic, New York, 1979), p. 460.
[46] R. López-Ruiz, H. L. Mancini, and X. Calbet, Phys. Lett. A **209**, 321 (1995).
[47] R. G. Catalán, J. Garay, and R. López-Ruiz, Phys. Rev. E **66**, 011102 (2002).
[48] R. López-Ruiz, Biophys. Chem. **115**, 215 (2005).
[49] J. C. Angulo and J. Antolín, J. Chem. Phys. **128**, 164109 (2008).
[50] R. O. Esquivel, J. C. Angulo, J. Antolín, J. S. Dehesa, S. López-Rosa, and N. Flores-Gallegos, Phys. Chem. Chem. Phys. **12**, 7108 (2010).
[51] T. Koga, K. Kanayama, S. Watanabe, and A. J. Thakkar, Int. J. Quantum Chem. **71**, 491 (1999).
[52] T. Koga, K. Kanayama, T. Watanabe, T. Imai, and A. J. Thakkar, Theor. Chem. Acc. **104**, 411 (2000).
[53] T. Koga, M. Omura, H. Teruya, and A. J. Thakkar, J. Phys. B **28**, 3113 (1995).
[54] N. H. March, Phys. Rev. A **33**, 88 (1986).